

New fluorescent auxin probes visualise tissue-specific and subcellular distributions of auxin in *Arabidopsis*

Barbora Pařízková^{1*} , Asta Žukauskaitė^{1*} , Thomas Vain^{2*} , Peter Grones^{2*} , Sara Raggi² ,
Martin F. Kubes^{1,3} , Martin Kieffer⁴ , Siamsa M. Doyle² , Miroslav Strnad¹ , Stefan Kepinski⁴ ,
Richard Napier³ , Karel Doležal^{1,5} , Stéphanie Robert²  and Ondřej Novák^{1,2} 

¹Laboratory of Growth Regulators, Faculty of Science, Palacký University and Institute of Experimental Botany, The Czech Academy of Sciences, Šlechtitelů 27, Olomouc CZ-78371, Czech Republic; ²Department of Forest Genetics and Plant Physiology, Umeå Plant Science Centre, Swedish University of Agricultural Sciences, Umeå SE-90183, Sweden; ³School of Life Sciences, The University of Warwick, Coventry, CV4 7AL, UK; ⁴Centre for Plant Sciences, University of Leeds, Leeds, LS2 9JT, UK; ⁵Department of Chemical Biology, Faculty of Science, Palacký University, Šlechtitelů 27, Olomouc CZ-78371, Czech Republic

Summary

Authors for correspondence:

Ondřej Novák

Email: novako@ueb.cas.cz

Stéphanie Robert

Email: stephanie.robert@slu.se

Received: 20 October 2020

Accepted: 21 December 2020

New Phytologist (2021) 230: 535–549

doi: 10.1111/nph.17183

Key words: *Arabidopsis*, distribution, fluorescent auxin, *in vivo* visualisation, subcellular localisation, transport.

- In a world that will rely increasingly on efficient plant growth for sufficient food, it is important to learn about natural mechanisms of phytohormone action. In this work, the introduction of a fluorophore to an auxin molecule represents a sensitive and non-invasive method to directly visualise auxin localisation with high spatiotemporal resolution.
- The state-of-the-art multidisciplinary approaches of genetic and chemical biology analysis together with live cell imaging, liquid chromatography–mass spectrometry (LC-MS) and surface plasmon resonance (SPR) methods were employed for the characterisation of auxin-related biological activity, distribution and stability of the presented compounds in *Arabidopsis thaliana*.
- Despite partial metabolism *in vivo*, these fluorescent auxins display an uneven and dynamic distribution leading to the formation of fluorescence maxima in tissues known to concentrate natural auxin, such as the concave side of the apical hook. Importantly, their distribution is altered in response to different exogenous stimuli in both roots and shoots. Moreover, we characterised the subcellular localisation of the fluorescent auxin analogues as being present in the endoplasmic reticulum and endosomes.
- Our work provides powerful tools to visualise auxin distribution within different plant tissues at cellular or subcellular levels and in response to internal and environmental stimuli during plant development.

Introduction

Auxin is a phytohormone with morphogen-like characteristics, which plays an essential role in controlling plant growth and development. The basic aspect of auxin action lies in its uneven distribution creating local concentration maxima in specific cells or tissues (Enders & Strader, 2016). Precise spatiotemporal auxin levels are regulated by auxin biosynthesis, active polar auxin transport (PAT) and conjugation and degradation processes (Ljung, 2013). This uneven auxin distribution together with auxin perception at the cellular level coordinates plant morphogenesis in response to exogenous and endogenous stimuli (Sauer *et al.*, 2013) during processes including embryogenesis, gravitropic and phototropic responses or lateral root and root hair formation (Vanneste & Friml, 2009).

Indole-3-acetic acid (IAA) is the most important naturally occurring auxin (Simon & Petrásek, 2010). Furthermore, a wide

range of small synthetic molecules with auxin activity has been described (Ma & Robert, 2014). Compounds such as 2,4-dichlorophenoxyacetic acid (2,4-D) or 1-naphthaleneacetic acid (NAA) are more stable compared with endogenous auxins and are widely used as growth regulators in research (Woodward & Bartel, 2005) and as herbicides in horticulture and agriculture. Auxin action is triggered via its perception by specific receptors controlling the expression of auxin-responsive genes. The best-described auxin perception system is based on auxin-dependent degradation of AUXIN/IAA INDUCIBLE (AUX/IAA) transcription repressors by the 26S proteasome. Binding of IAA to the TRANSPORT INHIBITOR RESPONSE 1 (TIR1) or AUXIN SIGNALLING F-BOX (AFB) receptors promotes the interaction of TIR1/AFB with AUX/IAA transcription inhibitors. The subsequent degradation of AUX/IAAs leads to the release of AUXIN RESPONSE FACTOR (ARF) transcription factors and expression of auxin-responsive genes (Lavy & Estelle, 2016).

IAA is a weak acid adopting a protonated form in the acidic environment of the apoplast that allows cellular uptake by passive

*These authors contributed equally to this work.

diffusion (Vieten *et al.*, 2007). In the neutral pH of the cytoplasm, IAA dissociates into a deprotonated form, reducing its passive transport through the plasma membrane (Adamowski & Friml, 2015), and active transport is therefore needed to generate cell-to-cell auxin flux (Lomax *et al.*, 1995). The tissue specificity and polar localisation of auxin influx and efflux carriers are essential in generating auxin maxima in specific tissues such as lateral root initiation sites in the root pericycle, the concave side of the apical hook or the quiescent centre (QC) of the root apex (Grones & Friml, 2015). The main protein family contributing to auxin uptake into the cell is AUXIN RESISTANT 1/LIKE AUX (AUX1/LAX) (Bennett *et al.*, 1996; Péret *et al.*, 2012), whereas PIN-FORMED (PIN) proteins act as auxin efflux facilitators (Adamowski & Friml, 2015). Moreover, the members of the ATP-binding cassette subfamily B (ABCB) also contribute to direct auxin transport (Geisler & Murphy, 2006). Among these, ABCB1 and ABCB19 act as auxin exporters (Zažímalová *et al.*, 2010), but the function of the close homologues ABCB4 and ABCB21 has been shown to be facultative (Mitchison, 2015). These homologues play a role as auxin influx carriers under low auxin concentrations, whereas in high auxin levels both ABCB4 and ABCB21 are converted to auxin efflux transporters (Kamimoto *et al.*, 2012; Kubeš *et al.*, 2012). In addition, PIN-like (PILS) putative auxin carriers (Barbez *et al.*, 2012) localised on endoplasmic reticulum (ER) membranes and vacuolar auxin transporter WALLS ARE THIN1 (WAT1) (Ranocha *et al.*, 2013) also participate in the maintenance of intracellular auxin homeostasis. However, auxin homeostasis at the subcellular level has not been easy to study even though organelle-specific auxin biosynthesis, metabolism and transport sites have been discovered (Skalický *et al.*, 2018). As specific ER and vacuolar auxin transporters have been identified, auxin is expected to be present in these organelles, although little information is known about the resting and active concentrations in these compartments. In protoplasts, auxin enters the nucleus predominantly via the ER (Middleton *et al.*, 2018) and IAA has been identified in endosomes and endomembranous compartments of root apex cells in maize (Schlicht *et al.*, 2006) and *Arabidopsis* (Mettbach *et al.*, 2017) by immunofluorescence or immunogold staining, respectively. Moreover, treatment with the endomembrane trafficking inhibitor brefeldin A (BFA) that traps auxin PIN transporters in endosomal vesicles and induces their intracellular accumulation (Steinmann *et al.*, 1999), resulted in a strong auxin signal in BFA-induced compartments (Schlicht *et al.*, 2006; Mettbach *et al.*, 2017). Overall, the importance of active auxin transport in plant development or in responses to environmental stimuli at both tissue and cellular levels has been demonstrated by the diverse developmental defects of mutants defective in auxin transport. For instance, proper apical hook development protects the shoot apical meristem while the seedling emerges through the soil and is highly dependent on tissue-specific auxin distribution mainly mediated by the auxin importer proteins AUX1 and LAX3 (Vandenbussche *et al.*, 2010) and PIN exporters, especially PIN3 (Žádníková *et al.*, 2010). This auxin transport machinery contributes to the formation of an auxin gradient with a maximum on the concave side of the hook (Vandenbussche *et al.*,

2010), resulting in differential growth between the inner and outer sides of the hypocotyl to form a hook-like structure (Abbas *et al.*, 2013). Exposure of the etiolated seedling to light results in PAT-mediated auxin redistribution from the concave side leading to apical hook opening (Schwark and Schierle, 1992; Lehman *et al.*, 2009).

2,4-D and NAA are useful tools for studying auxin transport as they can dissect auxin influx and efflux due to their different transport properties (Delbarre *et al.*, 1996; Lewis and Muday, 2009). The uptake of 2,4-D is predominantly facilitated by the AUX1/LAX auxin influx carriers (Delbarre *et al.*, 1996; Yang *et al.*, 2006; Péret *et al.*, 2012; Hoyerová *et al.*, 2018), whereas this compound is a poor substrate for auxin efflux carriers. By contrast, NAA transport is predominantly facilitated by PIN-mediated efflux, especially by PIN4 and PIN7 (Petrášek *et al.*, 2006). In addition, ABCB1 and ABCB19 contribute to the efflux of 2,4-D (Yang & Murphy, 2009) while ABCB4 facilitates the efflux of NAA (Cho *et al.*, 2007).

Several methods have been developed to study the regulation of auxin response distribution during plant development. Auxin-specific genetic reporters enable tissue-specific localisation of auxin activity as a result of the expression of markers (e.g. β -glucuronidase (GUS) or fluorescent proteins) fused to auxin-sensitive promoters (Pařízková *et al.*, 2017). In addition, degradation-based reporters have been constructed to provide sensitive and rapid responses to the presence of auxin at a cellular resolution. The fluorescently tagged DII domain of the AUX/IAA repressors (DII-Venus) undergoes rapid degradation in response to auxin (Tan *et al.*, 2007). The loss of the DII-Venus fluorescent signal can therefore be used to detect dynamic changes in auxin distribution (Brunoud *et al.*, 2012). Approaches employing microelectrodes, scintillation detection of radiolabelled IAA molecules or IAA targeted monoclonal antibodies all provide the potential for direct detection of auxin distribution in plants, but none has been widely adopted (Pařízková *et al.*, 2017). By contrast, auxin fluorescent labelling has recently become popular and this technique represents a real-time and relatively non-invasive approach for detecting auxin distributions directly *in vivo* (Hayashi *et al.*, 2014; Sokołowska *et al.*, 2014; Bielezová *et al.*, 2019).

Here we present new tools to monitor auxin distribution using 2,4-D analogues labelled with the 7-nitro-2,1,3-benzoxadiazole (NBD) fluorophore. These fluorescently labelled 2,4-D derivatives specifically accumulate in the tissues when auxin maxima are expected, such as the QC of root tips or concave side of apical hooks. Moreover, at a subcellular level, we discovered the presence of the fluorescent analogues in specific organelles: ER and endosomes. Such a toolset represents high spatiotemporal resolution support for revealing the mechanisms behind the precise, local regulation of auxin distribution in live material.

Materials and Methods

Plant materials and growth conditions

Seeds of *Arabidopsis thaliana* ecotype Columbia (Col-0) were sown on plates of half-strength Murashige & Skoog medium

($\frac{1}{2}$ MS) medium (2.2 g l^{-1} Murashige & Skoog medium Duchefa Biochemie, 1% sucrose, 0.05 g l^{-1} morpholinoethanesulfonic acid Sigma Aldrich and 0.7% agar Duchefa Biochemie, pH 5.6), stratified for 2 d at 4°C in the dark and then transferred to long-day light conditions (22°C , 16 h : 8 h, light : dark) for 5 d for light-grown seedlings. After 2 d of stratification and 5 h in light (22°C), sown plates were packed into aluminium foil and grown in the dark for 3 d for dark-grown seedlings. *aux1-21lax3* (Swarup *et al.*, 2008), *pD R5::GUS* (Ulmasov *et al.*, 1997), *p35S::DII-Venus* (Brunoud *et al.*, 2012), *pDR5rev:erRFP* (Marin *et al.*, 2010), *pSYP61::SYP61-CFP* (Robert *et al.*, 2008), *p35S::H2B-mCherry* (Mao *et al.*, 2016) and *p2485-RFP* (Montesinos *et al.*, 2012) Arabidopsis lines were on the Col-0 background and have been described before. The *pin3pin4pin7* mutant on the Col-0/*Ler* background was kindly provided by H el ene S. Robert, Ceitec, Brno, Czechia.

FluorA synthesis and metabolisation dynamics determination

For a detailed description of the synthesis of FluorA compounds and LC-MS/MS determination of their metabolisation dynamics *in planta* see the Supporting Information (Methods S1, S2; Eyer *et al.*, 2016). The GUS assay and surface plasmon resonance (SPR; Lee *et al.*, 2014) method were further employed for the characterisation of auxin-related biological activity (see Methods S3, S4, respectively). The storage and usage of the compounds are described in more detail in Notes S1.

p35S::DII-Venus auxin-responsive assay

Here, 5-d-old seedlings of *p35S::DII-Venus* Arabidopsis lines were treated in liquid $\frac{1}{2}$ MS medium in the presence of $10 \mu\text{M}$ fluorescent compounds or dimethyl sulphoxide (DMSO) and 230 nM 2,4-D as controls for 15 min. Treatment was followed by a 30-min washout of the compounds with fresh medium, which was changed three times during the washout step. The seedlings were then transferred to a glass slide with a drop of untreated medium and confocal images of Venus fluorescence were taken as described in the following section.

Imaging of fluorescent auxin analogues

Seedlings were typically treated by immersion in liquid $\frac{1}{2}$ MS medium supplemented by auxin fluorescent analogues at $2 \mu\text{M}$ concentration for 15 min, and then transferred to microscope glass slides with a drop of the medium containing tested compounds. Confocal images were taken immediately using a Zeiss LSM 780 confocal microscope with an LCI Plan-Neofluar $\times 25/0.8$ Imm Corr differential interference contrast (DIC) M27 objective. NBD-labelled auxins and Venus fluorescent protein were excited at 488 nm , red fluorescent protein (RFP) and mCherry fluorescent proteins at 560 nm and cyan fluorescent protein (CFP) at 458 nm by an argon multiline laser. For a detailed description of transport assay and subcellular localisation experiments see Methods S5.

Distribution assays of FluorAs in response to light or gravity

To test the distribution of fluorescent analogues in apical hooks, 3-d-old etiolated seedlings of Arabidopsis were treated with $2 \mu\text{M}$ fluorescent analogues in liquid medium under green light, kept in darkness for 15 min and then transferred to vertical plates containing solid $\frac{1}{2}$ MS medium supplemented with $2 \mu\text{M}$ compounds. Plates were placed vertically in a humidifying dark chamber to avoid drying of the samples and confocal images were immediately recorded (time point 0 min) with a Nikon vertical macroconfocal (AZ-C2 vertical) with a AZ100 horizontally mounted microscope with option of $\times 2/0.2 \text{ WD } 45 \text{ mm}$ or $\times 5/0.5 \text{ WD } 15 \text{ mm}$ DIC macro-objectives. After the first image, the control plates were maintained in darkness while the plates to be light-stimulated were transferred to a growth chamber under standard light conditions for 30 min before being imaged again (time point 30 min). The control plates maintained in darkness were imaged every 30 min for 90 min.

Next, 5-d-old seedlings of Arabidopsis grown on square plates were gravistimulated by 90° rotation for 40 min, then transferred to liquid medium in 24-well plates and treated with a $2 \mu\text{M}$ solution of fluorescent analogues for 15 min. The seedlings were then transferred to a glass slide and imaged using a Zeiss LSM 780 confocal microscope as described previously.

Statistical analysis

Measurements of NBD fluorescence intensity were performed using IMAGEJ v.1.51f software (Schindelin *et al.*, 2015). Statistical analysis of data was performed to compare treatment with DMSO control using two-sided independent Student's *t*-tests using EXCEL (Microsoft).

Image processing

All adjustments of acquired scanned or confocal images were performed using IMAGEJ v.1.51w software (Schindelin *et al.*, 2015) with the same settings for each experimental dataset. Drawings were accomplished by CHEMBIODRAW ULTRA, CORELDRAW X7 and Adobe ILLUSTRATOR.

Results

Design strategy for generation of the fluorescent auxin library

The intention of this study was to develop fluorescently labelled auxins that would maintain the original hormone activity and would display auxin-like distribution in plant tissues. As the influx of 2,4-D *in planta* is primarily achieved via AUX1, this compound has long been used to study auxin influx mechanisms (Seifertov a *et al.*, 2014). Additionally, 2,4-D was recently shown to be transported via auxin exporters (Yang & Murphy, 2009) and shows lower sensitivity to inactivating enzymes compared with IAA *in planta* (Grossmann, 2009), making it a credible reporter molecule for auxin transport research. Our parallel study

(Vain *et al.*, 2019) demonstrated that 2,4-D analogues bearing various phenylpiperazines or phenylthioethylamines coupled via an amide bond to their carboxyl group appeared to promote specific interactions of the auxin receptor TRANSPORT INHIBITOR RESPONSE1 (TIR1) with different AUX/IAA transcriptional regulators to influence different developmental processes.

Inspired by these results, 2,4-D was fluorescently labelled with an NBD fluorophore via its carboxyl group using three different linkers – ethylenediamine (EDA), piperazine (PIP) and 1,3-dimercaptopropane (DMP) and the resulting compounds were collectively named FluorAs (from fluorescent auxins) (Fig. S1a; Methods S1). Based on a screening strategy (Fig. S1b), EDA and PIP linkers were then chosen to label other auxin analogues (4-bromophenoxyacetic acid, 4-Br-POA; 2,4,5-trichlorophenoxyacetic acid, 2,4,5-T; 4-chlorophenoxyacetic acid, 4-Cl-POA and 2-phenoxyacetic acid, POA) with an NBD tag (Fig. S1a) to obtain a wide portfolio of fluorescent auxin reporter candidates.

Searching for candidates – the structure–activity relationships of FluorAs

The best candidate FluorAs were chosen based on their biological activity and fluorescent properties *in planta* (Figs 1, S1b). Their activity was established by their ability to inhibit primary root growth of *Arabidopsis* Col-0 seedlings (Figs 1a, S2a,b) and to

induce the expression of *Arabidopsis* auxin response marker *pDR5::GUS* (Fig. S2c; Methods S3). The most active fluorescent analogues were the ones derived from 2,4-D (FluorA I–III) regardless of the linker, showing a dose-dependent bioactivity above 1 μM on primary root growth (Figs 1a, S2b; Table S1) and promoting the expression of *pDR5::GUS* in roots at 10 μM within 5 h of treatment (Fig. S2c). Other fluorescent derivatives exhibited lower or no activity in both assays (FluorA IV–XI; Fig. S2a–c), except FluorA IX, a 4-Cl-POA derivative, that displayed an effect similar to the 2,4-D-like compounds. However, as FluorA IX induced a different biological response to FluorA VIII, the other 4-Cl-POA analogue tested, we chose to exclude FluorA IX from the candidates. In addition, the fluorescence properties of the 2,4-D analogues FluorA I, II and III, bearing three different linkers (EDA, PIP and DMP) (Fig. S1a) were evaluated. FluorA XI derived from POA, which did not affect root growth or *pDR5::GUS* expression (Fig. S2a–c), was suitable as a negative control. The strongest fluorescent signal was provided by FluorA II (Figs 1b, S3). Using the confocal settings and treatment parameters optimised for FluorA II (Fig. S3a,b), FluorA I and XI displayed a similar distribution pattern to FluorA II but showed lower fluorescence intensity in roots after 15 min uptake at 2 μM (Figs S3a,b, S4a). Unfortunately, FluorA III, the most active analogue in the auxin bioassays (Fig. S2b,c), did not provide any fluorescent output (Fig. 1b), appearing similar to DMSO control (Fig. S4b), making this compound unsuitable for

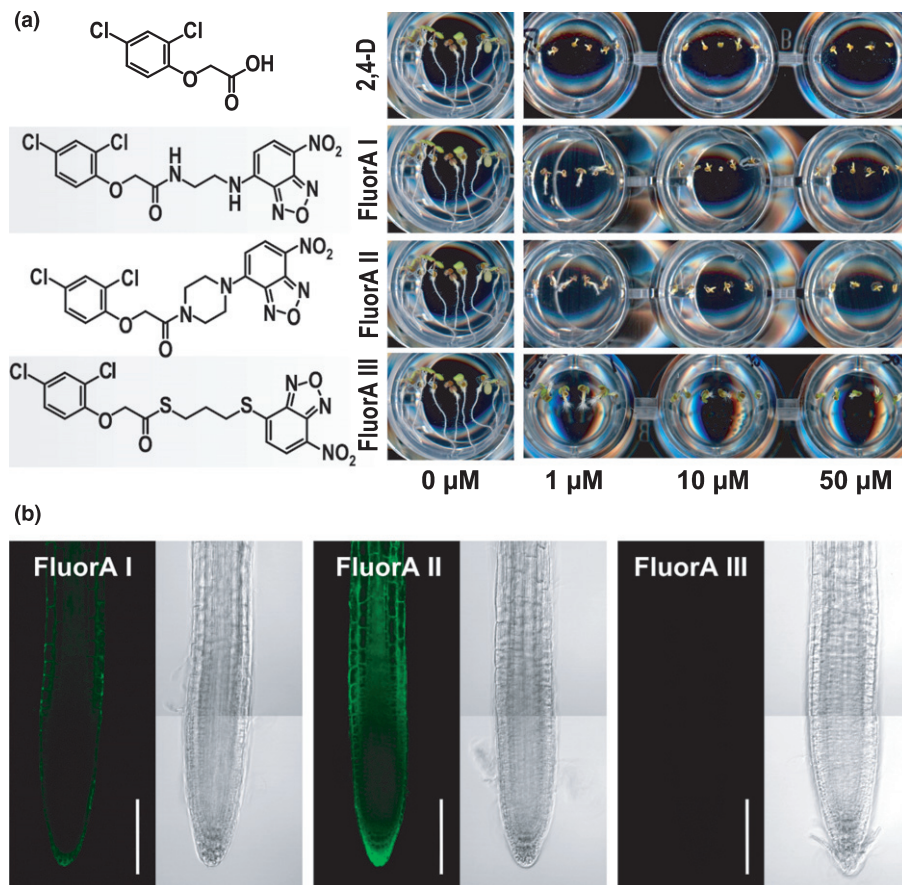


Fig. 1 Screening strategy for FluorAs. (a) Dose-dependent effect (1, 10, 50 μM) of 2,4-dichlorophenoxyacetic acid (2,4-D) and FluorA compounds or dimethyl sulfoxide (DMSO) only (0 μM) on primary root growth of *Arabidopsis thaliana* Col-0 wild-type (WT). (b) Accumulation of FluorA compounds in the primary root of *Arabidopsis* Col-0 WT. The fluorescence signal was visualised with confocal settings optimised for FluorA II. Bars, 100 μm .

visualising auxin distribution. Moreover, PIP-NBD (the linker and fluorophore of FluorA II but lacking the 2,4-D moiety) was not taken up (Fig. S4b), so the uptake of the compounds appeared to be dependent on the auxinic substructure. Our compound screening revealed that FluorA I and FluorA II were two promising fluorescent candidates derived from 2,4-D and suitable for advanced characterisation of their biological functions.

Biological activity of FluorAs related to their metabolism *in planta*

As these results suggested that the 2,4-D-derived FluorA analogues actively affected plant growth in an auxin-dependent manner, as well as triggering an early auxin-responsive promoter, we investigated their uptake and stability dynamics *in vivo*. For this purpose, a rapid analytical approach using a one-step purification method coupled with liquid chromatography-tandem mass spectrometry (LC-MS/MS) was developed to perform absolute quantification of all analytes (Methods S2). To address the observed biological activity to FluorA compounds, this method was employed for determination of time-dependent metabolism dynamics of fluorescent 2,4-D derivatives in roots of Arabidopsis Col-0 seedlings. In the time-course experiment, a linear trend of FluorA metabolism to free 2,4-D was observed (Fig. 2a,b; Table S2). It was calculated that after 15 min of 10 μ M FluorA treatment *c.* 2.7 pmol of free 2,4-D was released per 50 roots. To calculate the exogenous concentration of 2,4-D providing this amount of internal 2,4-D, we performed a dose–response analysis on Col-0 wild-type (WT) seedlings with various 2,4-D concentrations. The quantification of 2,4-D levels accumulated internally upon 15 min of treatment (Fig. 2c; Table S3) led us to estimate the appropriate treatment concentration of 2,4-D as 230 nM using the determined quadratic equation. Seedlings of the Arabidopsis reporter line *p35S::DII-Venus*, which expressed fluorescently labelled auxin-sensitive DII domains of AUX/IAAs, were then treated for 15 min with 10 μ M FluorA compounds and 230 nM 2,4-D, and the fluorescence signals in response to the treatments were compared (Fig. 2d). The quantification of the Venus signal showed that these treatments led to similar levels of degradation of the Venus signal (Fig. 2e; Table S4). This strongly suggested that the observed auxinic activity came from metabolism of FluorAs to 2,4-D. This fact was also supported by the SPR analysis (Methods S4), which revealed that FluorA derivatives did not bind to the TIR1 receptor *in vitro* and therefore did not display auxin activity, and only a very weak anti-auxin activity, as FluorA II slightly inhibits IAA-TIR1 binding (Fig. 2f,g; Dataset S1). Therefore, we can assume that FluorA compounds are not perceived by the auxin perception machinery and that the biological activity previously observed in auxin bioassays should be addressed to free 2,4-D released by *in vivo* metabolism of FluorAs.

Localisation of FluorAs *in planta*

Even though the biological activity of FluorAs was difficult to assess, we tested their potential as tools for dissecting the auxin

transport machinery activity. Hence, the *in planta* localisation of FluorA I and II, as well as XI as a negative control, was further investigated in both shoots and roots of Arabidopsis (Methods S5).

The DMSO control showed no specific fluorescent pattern in the shoots of dark-grown seedlings (Fig. S4c), but the FluorA I signal was visible at the base of the cotyledons, and an uneven distribution of FluorA II was observed in the apical hook region of the hypocotyl (Fig. 3a), reminiscent of the asymmetric auxin distribution known to occur across the hook, with accumulation in the concave side (Žádníková *et al.*, 2010). The marked auxin-like distribution of FluorA II in the apical hook was further analysed in etiolated *pDR5rev:erRFP* seedlings, in which a similar pattern of localisation was observed for RFP and NBD signals after FluorA II but not DMSO treatment (Fig. 3b). Importantly, FluorA XI did not show any such accumulation pattern in the apical hook (Fig. S4c).

In the root, both FluorA I and II displayed accumulation in the epidermis, QC of the root tip, columella and lateral root cap (Fig. 3c). Moreover, these 2,4-D probes were also detected in lateral root primordia in the early stages of development but with no obvious preferential accumulation (Fig. 3d). In early-emerging lateral roots, FluorA I, unlike FluorA II, displayed auxin-like accumulation (Benková *et al.*, 2003) with the strongest signal at the emerging tip (Fig. 3e).

To conclude, even though FluorAs are slightly metabolised *in vivo*, they can serve as convenient tools to non-invasively visualise tissue-specific auxin localisations in a complementary manner in plants.

Auxin transport carriers are involved in distribution of FluorAs

We next examined the impact of auxin transport mechanisms on the distribution of FluorAs in Arabidopsis. The pretreatment of plants with the auxin efflux inhibitor *N*-1-naphthylphthalamic acid (NPA) led to the cellular accumulation of both FluorA I and II in roots, increasing the overall fluorescence signal (Fig. 4a; Table S5), which suggested that active auxin efflux is involved in regulating the distribution of these FluorA compounds. NPA treatment resulted in a pronounced fluorescent signal in the columella and the root cap cells of the root meristem and in the epidermis, however NPA-treated roots showed no accumulation in the QC (Fig. 4a). Importantly, NPA pretreatment did not lead to increased accumulation of FluorA XI (Fig. S4d), indicating that this compound is not actively exported, in contrast with FluorA I and II. No significant changes in fluorescence intensity or pattern were observed after affecting auxin influx pathways by using either the *aux1-21lax3* auxin transport mutant or pretreatment with the auxin influx inhibitor 2-naphthoxyacetic acid (2-NOA) (Fig. S4e; Table S6) indicating that the compounds are likely to bypass active auxin influx, and instead are internalised by passive diffusion.

A similar result was observed in the shoot during hypocotyl transport assays, in which decapitated etiolated hypocotyls were placed below blocks of agar containing 2 μ M FluorAs. After 3 h,

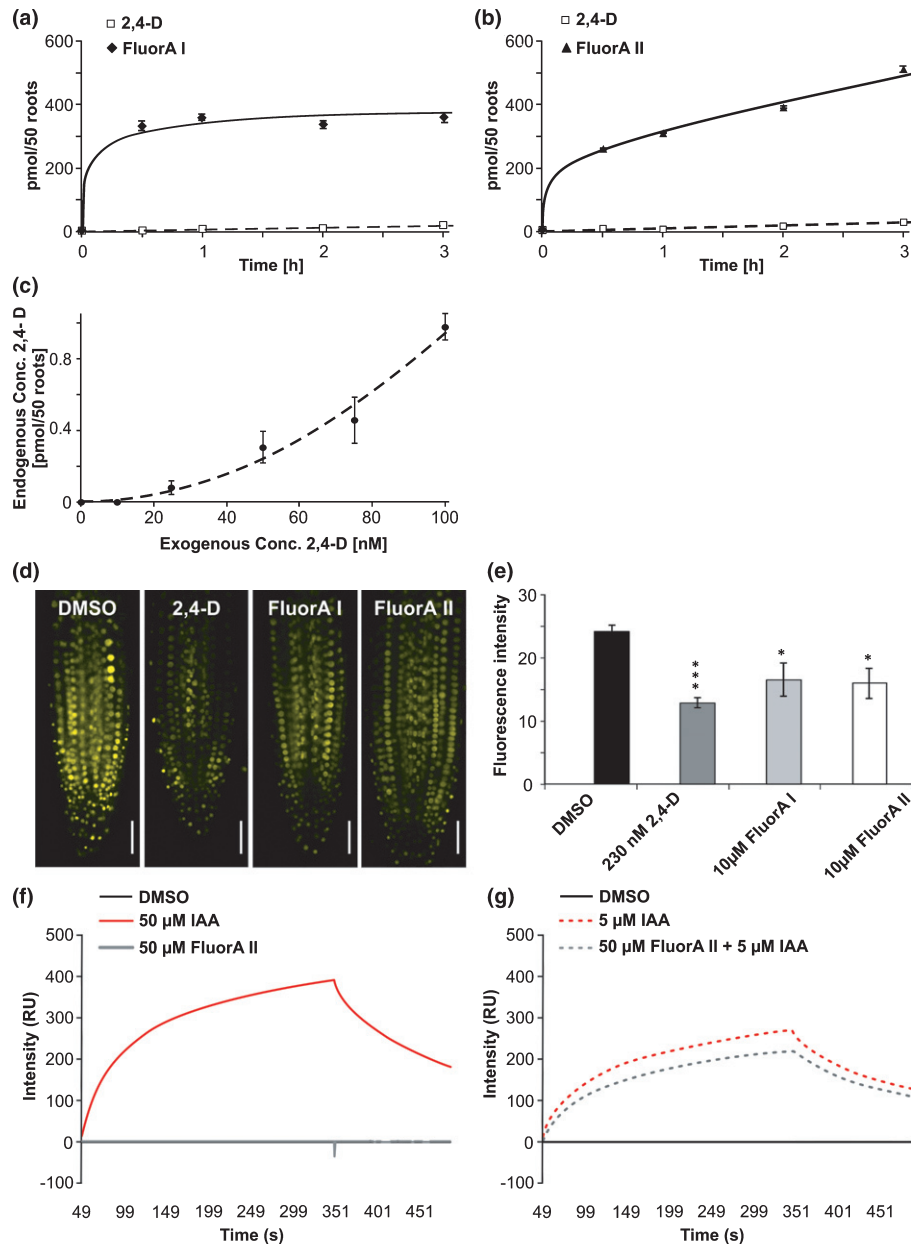


Fig. 2 Biological activity of FluorAs is driven by metabolism *in vivo*. (a, b) Quantitative determination of uptake and metabolism dynamics of FluorA I and FluorA II *in planta* using liquid chromatography–mass spectrometry (LC-MS/MS) detection. Seedlings of *Arabidopsis thaliana* Col-0 wild-type were treated in liquid $\frac{1}{2}$ MS medium supplemented with 10 μ M FluorA I (a) or FluorA II (b) and then roots were collected at defined time points. Both FluorA I and FluorA II displayed similar linear rates of metabolism and the linear equation was used to calculate free 2,4-dichlorophenoxyacetic acid (2,4-D) in 15 min to be 2.7 pmol/50 roots. Values are means \pm SD ($n = 4$). (c) Determination of internal levels of 2,4-D with respect to applied exogenous concentrations after 15 min uptake. The obtained quadratic equation was used for calculation of exogenous 2,4-D concentration for obtaining 2.7 pmol/50 roots *in planta* to be 230 nM. Values are means \pm SD ($n = 4$). (d) Representative images of *Arabidopsis p35S::DII-Venus* seedlings after 15 min treatment with dimethyl sulfoxide (DMSO), 230 nM 2,4-D and 10 μ M FluorA compounds. Bars, 50 μ m. (e) Quantification of Venus signal in the roots from experiment presented in (d), revealing that 2,4-D and FluorA treatments displayed similar auxin response suggesting that the bioactivity of FluorA compounds is caused by metabolism of FluorAs *in planta* to free 2,4-D. Statistical analyses were performed using the Student's *t*-test to compare with DMSO (values are means \pm SE; $n = 30$ from three independent biological replicates; *P*-values: *, $P < 0.05$; ***, $P < 0.0005$). (f, g) By recording the assembly of the TRANSPORT INHIBITOR RESPONSE 1/AUXIN SIGNALLING F-BOX (TIR1/AFB) and AUXIN/INDOLE-3-ACETIC ACID7 (IAA7) co-receptor complex, surface plasmon resonance (SPR) analysis confirmed that FluorAs do not possess auxin activity *in vitro* (a), but may exhibit very weak anti-auxin activity by competing with indole-3-acetic acid (IAA) and reducing the signal amplitude when present in excess (b). Traces for both FluorA I and FluorA II were comparable, therefore only results for 50 μ M FluorA II are presented.

fluorescence signals of both compounds were observed in the hypocotyl with a gradient distribution, being most concentrated near the agar block (Fig. S4f). NPA pretreatment of the

hypocotyls to block active auxin efflux did not prevent the FluorAs from entering the hypocotyls and the tissue signal pattern was similar to that in non-NPA-treated plants (Fig. S4f).

However, NPA treatment led to an increased signal close to the agar blocks, suggesting that both diffusion and PAT contributed to FluorA distribution. Moreover, in the apical hook regions of nondecapitated hypocotyls, the accumulations of FluorA I at the base of the cotyledons and FluorA II on the concave side of the apical hook were abolished by NPA treatment (Fig. 4b compared with Fig. 3a), showing that active auxin transport is required to create these maxima.

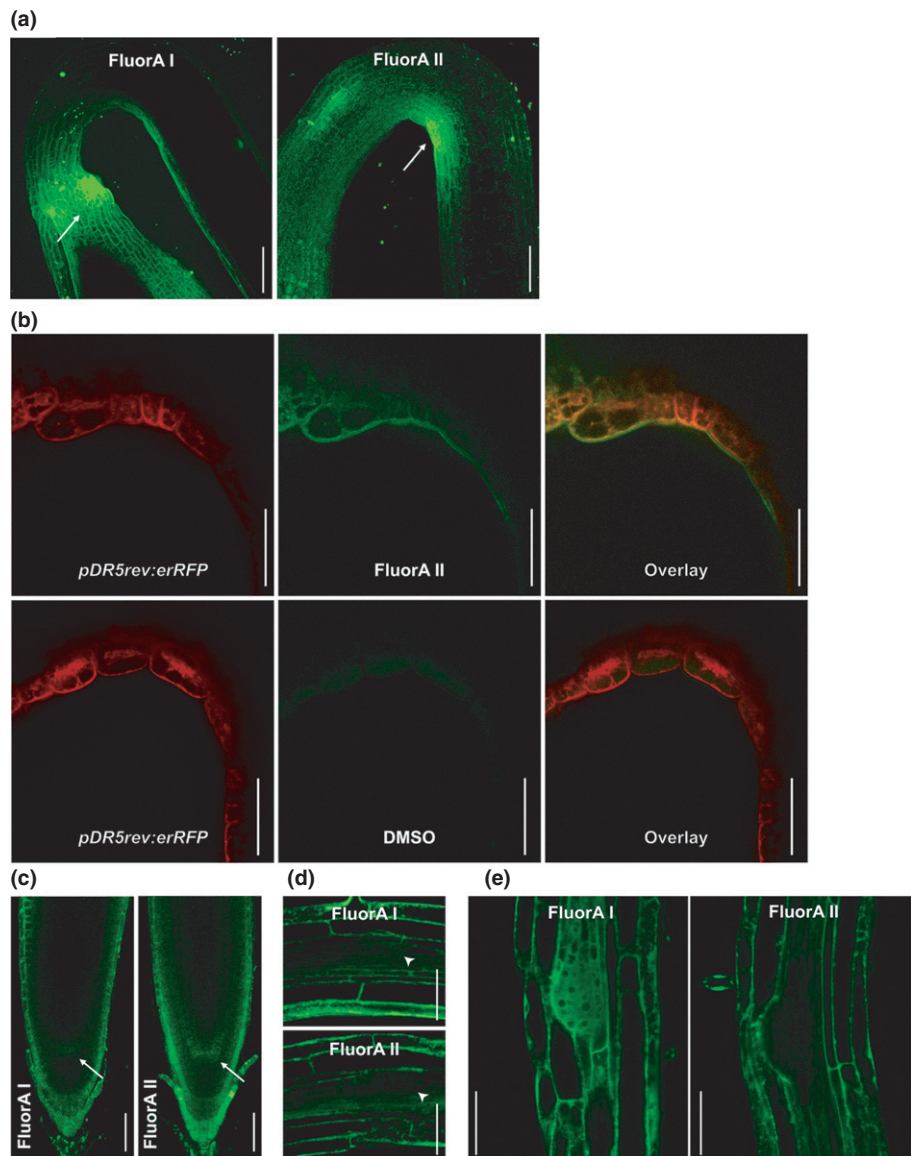
To explore the mechanisms of FluorA transport further, uptake and accumulation of FluorA II in auxin transport protein defective mutants were tested. In the *aux1-21lax3* mutant in Col-0 background that is deficient in two of the main auxin influx carriers, FluorA II accumulation in the concave side of the hook was abolished (Fig. 4c). Conversely, the *pin3pin4pin7* mutant in Col-0/*Ler* background, that lacks any hook-like structure, showed symmetrical accumulation of FluorA II in the epidermis on both sides of the hypocotyl (Fig. 4c), suggesting that PIN

proteins play an important role in the distribution of FluorA II. Markedly, the FluorA II signal was stronger in *Ler* compared with Col-0 wild-type (Fig. 4c). Overall, the data obtained indicated that the tissue distribution of both FluorA I and II is facilitated by diffusion and regulated by the active auxin transport system, allowing the use of these fluorescent analogues to visualise auxin distribution and auxin-dependent processes such as hook development in a precise way.

FluorAs allow visualisation of auxin redistribution following exogenous stimuli

PAT also plays an important role in auxin tissue-specific redistribution as a response to different kinds of environmental stimuli such as gravistimulation or light (Friml *et al.*, 2002; Adamowski & Friml, 2015). In agreement with this, roots of *Arabidopsis* Col-0 wild-type treated with FluorA I displayed an uneven

Fig. 3 Localisation of FluorAs in *planta*. (a) After 15 min treatment with 2 μ M concentration, FluorA I accumulated at the base of the cotyledons while FluorA II accumulated in the inner apical hook of 3-d-old dark-grown *Arabidopsis* Col-0 wild-type (WT) seedlings. The arrows indicate tissue-specific accumulation of FluorAs in the cotyledons or hypocotyl. Bars, 100 μ m. (b) Etiolated *Arabidopsis pDR5rev:erRFP* seedlings were treated with 2 μ M FluorA II or equivalent volume of DMSO for 15 min. RFP signal displayed similar localisation with 7-nitro-2,1,3-benzoxadiazole (NBD) signal on the concave side of the apical hook after FluorA II but not dimethyl sulfoxide (DMSO) treatment. Bars, 50 μ m. (c) FluorA I and FluorA II established concentration maxima in the epidermis, quiescent centre (QC), columella and lateral root cap of *Arabidopsis thaliana* Col-0 WT seedling roots after incubation with 2 μ M FluorAs for 15 min followed by transfer on untreated solid medium for 3 h. The arrows indicate QC cells. Bars, 50 μ m. (d, e) The presence of FluorAs in lateral root primordia (d) and emerging lateral roots (e) of *Arabidopsis* Col-0 WT seedlings after 15 min treatment with 2 μ M (d) or 10 μ M (e) FluorAs. The arrowheads indicate lateral root initiation sites. Bars, 50 μ m. Here, 10–13 seedlings per each of three biological replicates were observed and the frequency of those showing the specific FluorA accumulation presented was c. 80% (a) or 50% (c).



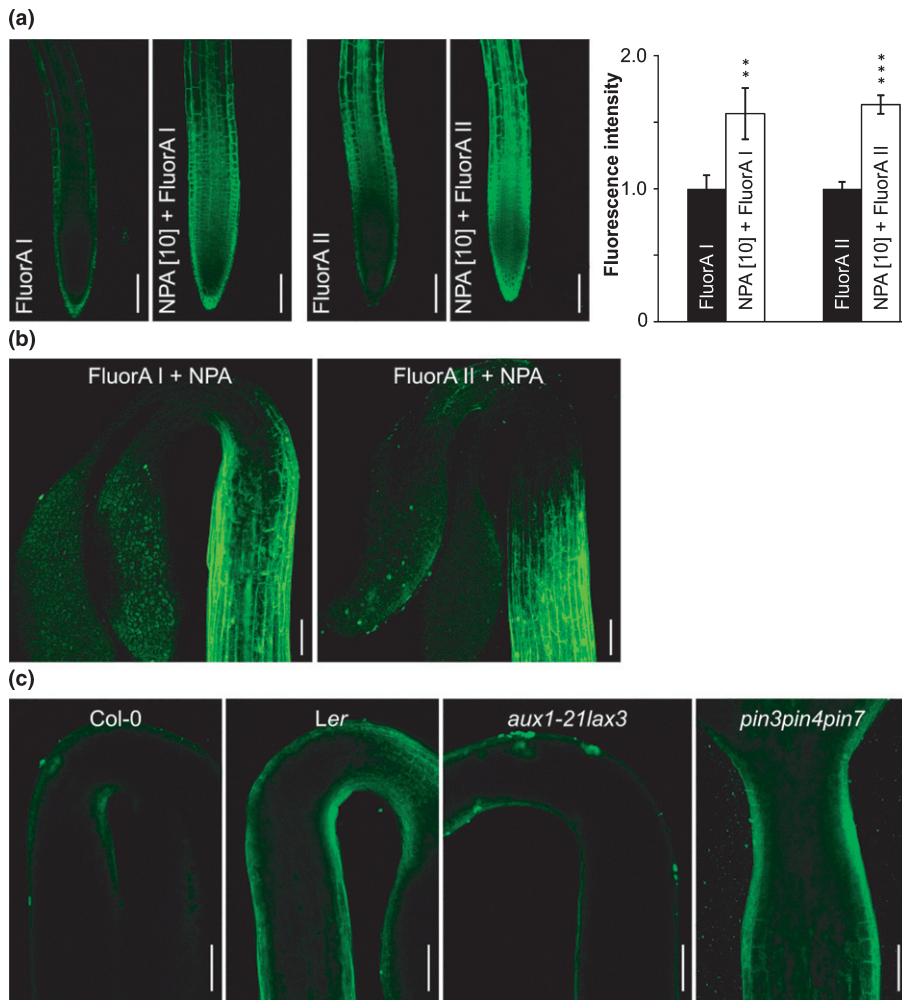


Fig. 4 Distribution of FluorAs *in planta* driven by polar auxin transport (PAT). (a) Auxin active transport inhibitor *N*-1-naphthylphthalamic acid (NPA) increases the intracellular accumulation of FluorA compounds. The intensity of the FluorA fluorescence in *Arabidopsis thaliana* roots was quantified and expressed relative to non-NPA-treated plants. Statistical analyses were performed using the Student's *t*-test to compare NPA-treated with untreated plants (values are means \pm SE; $n = 30$ from three independent biological replicates; *P*-values: ***, $P < 0.0001$). (b) NPA pretreatment disturbed the localisation of FluorA I in cotyledons and FluorA II in apical hooks of 3-day-old dark-grown *Arabidopsis Col-0* wild-type (WT) seedlings. Bars, 50 μ m. Here, 10–13 seedlings per each of three biological replicates were observed and the frequency of those showing the specific FluorA accumulation presented was *c.* 80%. (c) FluorA II displayed asymmetric distribution in both Col-0 and Ler WT apical hooks. The accumulation on the concave side was absent in the *aux1-21lax3* mutant while the *pin3pin4pin7* mutant lacking a hook-like structure exhibited symmetrical fluorescence signal in the epidermis on both sides of the hypocotyl. Bars, 100 μ m. For each genotype, 10–13 seedlings per each of three biological replicates were observed and the frequency of those showing the specific accumulation presented was *c.* 80% for each.

distribution of fluorescence in the epidermis following gravistimulation, with a slightly but consistently stronger signal on the lower side of the gravistimulated root (Fig. 5a), while the negative control FluorA XI did not show this effect (Fig. S4g). It has been shown that the differential accumulation of auxin in the apical hook is disrupted by light, leading to apical hook opening (Liscum & Hangarter, 1993). To test whether FluorA compound distribution was also sensitive to an external light signal, etiolated Col-0 wild-type seedlings with established fluorescent maxima of FluorA II on the concave side of the apical hook were transferred to standard light conditions and imaged at different time points. Control plants were kept in the dark. Continuous light stimulation led to the redistribution of the fluorescent signal and loss of accumulation at the concave side of the hook after 30 min (Fig. 5b), while the FluorA II accumulation was still observed at this 30 min time point in the seedlings incubated in the dark (Fig. 5c). However, 90 min after taking the first image, the accumulation had also disappeared in the dark-incubated seedlings (Fig. 5c). This redistribution in darkness might be a result of FluorA diffusion together with active transport from the hook zone caused by brief illumination during the imaging. Nevertheless, as it took a significantly longer time to lose the fluorescence accumulation in the dark-incubated compared with light-

stimulated seedlings, we proposed that the FluorA redistribution is triggered by light and is PAT dependent. Moreover, the consistent fluorescence signal in the roots at the same time points confirmed that the loss of accumulation was tissue specific, and not due to light-stimulated degradation of FluorA II (Fig. S5). Overall, our data showed that the fluorescently labelled auxin analogues FluorA I and FluorA II can be used as probes for visualisation of auxin sites of action and to follow auxin redistribution patterns during different developmental processes such as gravistimulation-induced root bending or light-induced apical hook opening.

High spatial resolution of FluorA imaging enables the study of subcellular auxin localisation

A huge advantage of fluorescently labelled hormones is the possibility of determining their distribution at high spatiotemporal resolution. Whereas other commonly used methods usually provide qualitative information about hormone distribution with an organ/tissue-level resolution, visualisation of small fluorescent molecules in real time is possible even at the subcellular level in a minimally invasive manner (Lace & Prandi, 2016). To investigate the distribution of FluorA I and II compounds at the level of

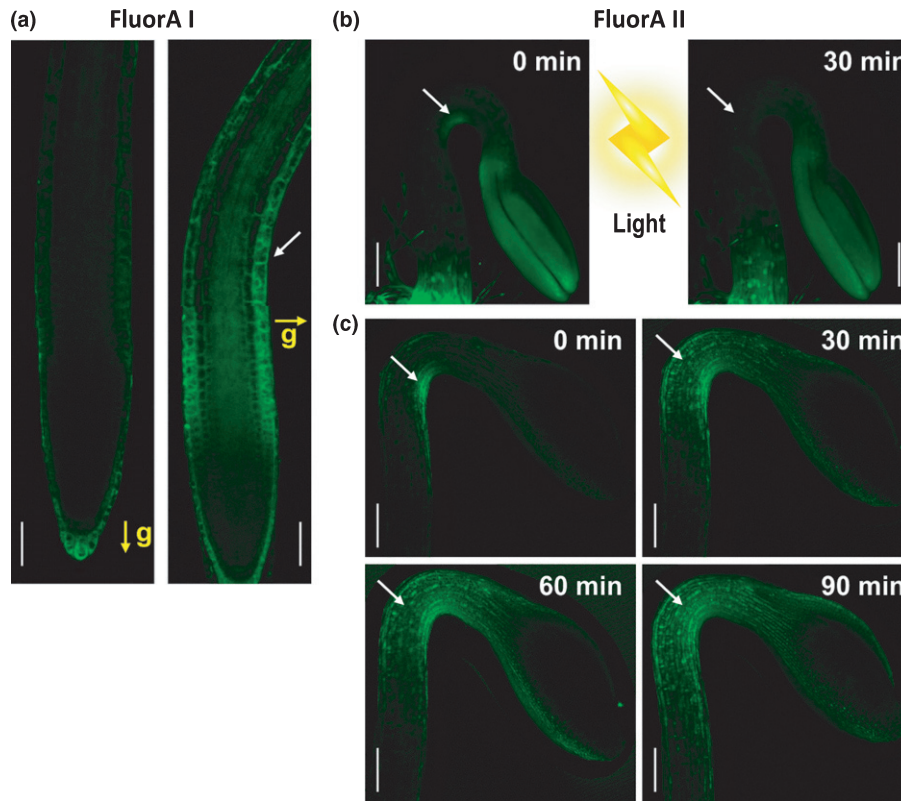


Fig. 5 Distribution of FluorAs in response to auxin-responsive external stimuli. (a) FluorA I accumulated asymmetrically in the gravistimulated roots of *Arabidopsis thaliana* Col-0 wild-type (WT) seedlings 40 min after the stimulation (right image) compared with nongravistimulated roots (left image). Bars, 100 μ m. Here, 10–13 gravistimulated seedlings per each of three biological replicates were observed and the frequency of those showing the specific accumulation presented was c. 60%. The white arrow indicates tissue-specific accumulation of FluorA I in gravistimulated root; yellow arrows indicate root orientation towards gravity (g). (b, c) Dark-grown seedlings of *Arabidopsis* Col-0 WT were treated in liquid $\frac{1}{2}$ MS medium supplemented with 2 μ M FluorA II, after 15 min they were transferred onto vertical plates containing solid $\frac{1}{2}$ MS medium supplemented with 2 μ M FluorA II and directly imaged with a vertical macroconfocal microscope (0 min). After that, the plates were either placed into an illuminated growth chamber (b) or kept in the dark (c) and imaged every 30 min. The FluorA II accumulation was redistributed after 30 min (b) and 90 min (c) with or without a continuous light stimulus, respectively. Bars, 1 mm. The white arrows indicate the concave apical hook side. Here, 10–13 seedlings per each of three biological replicates were observed in light and darkness and the frequency of seedlings showing the specific accumulation presented was c. 80% for each.

individual organelles, several *Arabidopsis* marker lines were examined for the co-localisation of the FluorA NBD signal with the fluorescent label of the respective organelle. The co-localisation of FluorA I and FluorA II with the (CFP)-tagged trafficking marker SYNTAXIN OF PLANTS 61 (*pSYP61::SYP61-CFP*) indicated the presence of FluorAs in the endosomes (Fig. 6a). In addition, both of the FluorAs showed higher co-localisation of the NBD signal with the SYP61 marker after treatment with BFA (Fig. 6b). These results suggested that the FluorA compounds localised to the endosomes within the endomembrane trafficking system. Moreover, the FluorA signals co-localised well with the p2485-RFP signal of an ER marker line, showing that both FluorA I and FluorA II localised to the ER (Fig. 6c). Conversely, under our experimental conditions the presence of FluorA compounds was not observed in the regions of condensed heterochromatin in the nucleus visualised with the *p35S::H2B-mCherry* marker (Fig. 6d). The presence of FluorA XI in ER and endosomes (Fig. S6) suggested partially passive transport of FluorA compounds to these organelles. Taken together, our results showed that our compounds can serve as useful research

tools to track the dynamics of the transport and distribution of auxins *in planta*, not only within different tissues, but also at the subcellular level.

Discussion

Recently, an extensive interest in imaging of signalling molecules has developed in the plant biology field (Lace & Prandi, 2016). Fluorescent versions of native and synthetic auxins, resulting in both fluorescently labelled (Muscolo *et al.*, 2007; Hayashi *et al.*, 2014; Sokołowska *et al.*, 2014; Bielezová *et al.*, 2019) and caged auxins (Atta *et al.*, 2010, 2013, 2015) have been reported and used for various purposes. The first attempt to label auxin for live imaging was performed by Sokołowska *et al.* N1 substitution of IAA was utilised for conjugation with fluorescein isothiocyanate (FITC) or rhodamine isothiocyanate (RITC) using a simple synthetic procedure. Both conjugates were shown to maintain auxin biological activity on oat coleoptiles and *Arabidopsis* roots as well as the native auxin distribution pattern in the latter (Sokołowska *et al.*, 2014). However, the stability of the compounds *in vivo*

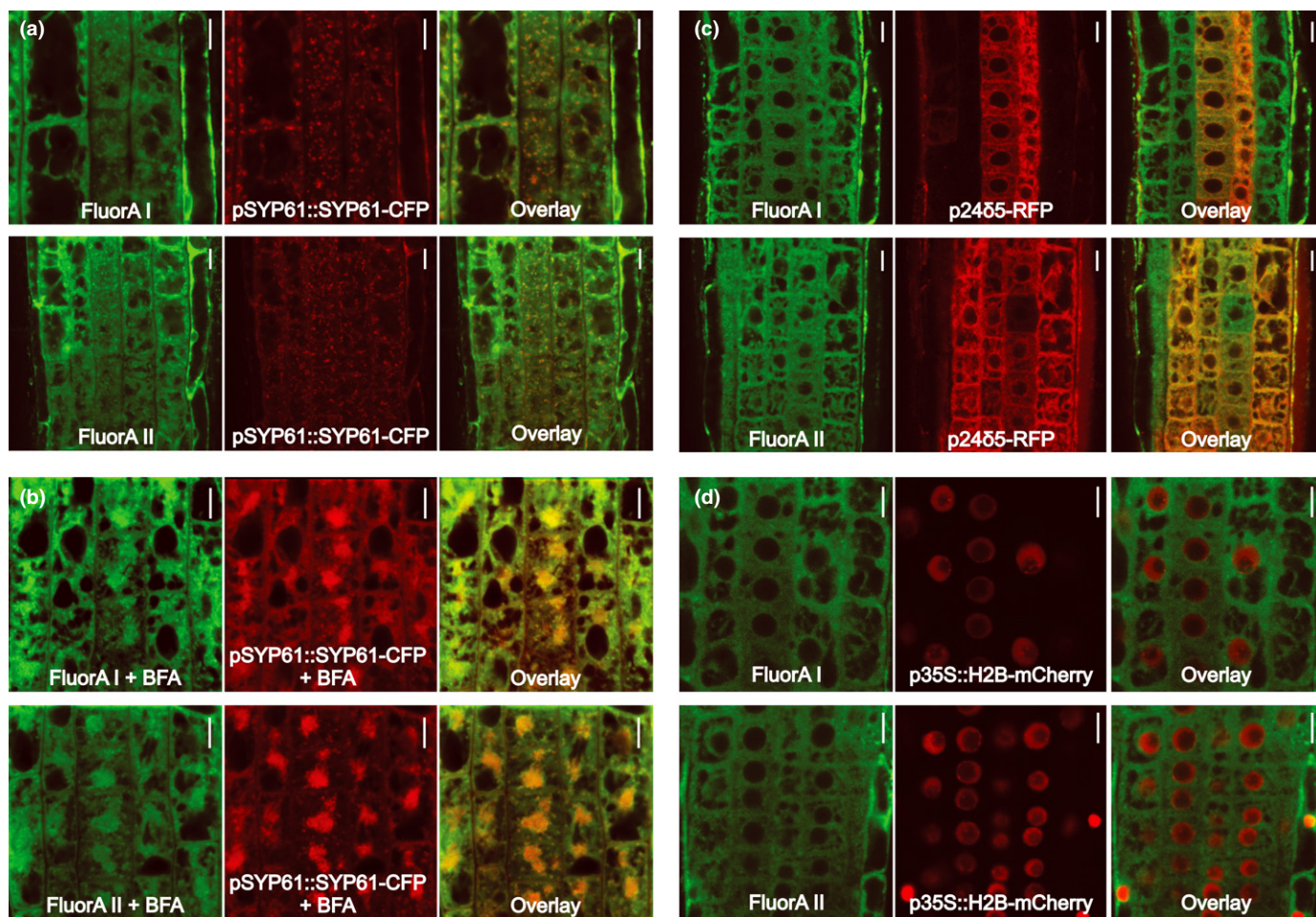


Fig. 6 Subcellular localisation of FluorAs. (a–d) Confocal images of epidermal cells of the root meristematic zone of *Arabidopsis thaliana* Col-0 seedlings expressing specific organelle markers indicate FluorA I and II to be localised in endosomes (a, b) without (a) and with (b) brefeldin A (BFA) treatment based on co-localisation of FluorA NBD fluorescence signal with *pSYP61::SYP61-CFP* marker; in endoplasmic reticulum (ER) (c) based on co-localisation of NBD signal with *p24δ5-RFP* marker; and in nuclei (d) based on co-localisation of 7-nitro-2,1,3-benzoxadiazole (NBD) signal with *p35S::H2B-mCherry* marker after 15 min treatment with 2 μ M FluorA compounds. Bars, 10 μ m. The focal plane was adjusted to capture particular organelles. The fluorescence intensity was digitally enhanced for FluorA I to improve visibility.

and its link with the auxin effects *in planta* were not discussed. By contrast, Hayashi and colleagues argued that elevated auxin concentrations would induce changes in auxin metabolism, such as an increase in GRETCHEN HAGEN 3 (GH3) auxin-inactivating enzymes (Ludwig-Müller, 2011) and alter the localisation of PIN transporters (Petrásek & Friml, 2009) and therefore the exogenous application of active fluorescent analogues would no longer mimic native auxin distribution. The authors, therefore, employed a synthesis strategy using benzyl-auxin analogues of IAA and NAA, which appeared to be recognised by auxin transporters but not by auxin receptors (Tsuda *et al.*, 2011). They focused on the preparation of two conjugates of IAA and NAA with NBD, which are active within the auxin transport system but inactive within auxin signalling (Hayashi *et al.*, 2014). Furthermore, a group of novel IAA fluorescent derivatives was prepared by introducing the NBD tag on the N1 position of the IAA indole ring via aliphatic linkers varying in the number of carbons in their structure from C₃ to C₆ (Bielešová *et al.*, 2019). Interestingly, such a substitution in the N1 position was shown

to change the auxin-like compound into an anti-auxin. Moreover, both the anti-auxin activity and fluorescence properties of these compounds were significantly dependent on the length of the linker, with the compound bearing the longest C₆ linker acting as the most potent anti-auxin as well as providing the best fluorescence properties (Bielešová *et al.*, 2019).

Here we present fluorescent auxin analogues derived from 2,4-D and labelled with NBD using two different linkers that are attached via the side-chain carboxyl group of the 2,4-D with an amide bond. Our concurrent study presenting structures similar to FluorA compounds, being 2,4-D and 2,4,5-T derivatives bearing the same PIP linker and a cysteamine aliphatic linker, showed these structures to be sterically favourable for binding to the TIR1-AUX/IAA7 co-receptor system in pull-down assays (Vain *et al.*, 2019). An extensive SPR analysis revealed that various auxin agonists, including chlorinated auxin derivatives, can differently stabilise the co-receptor system depending on the F-box-AUX/IAA partners, but that IAA conjugates were inactive (Lee *et al.*, 2014). Use of the same SPR assay revealed that none of the

FluorA conjugates of 2,4-D bound to the TIR1 receptor *in vitro*. Therefore, similarly to Hayashi's compounds, the FluorAs do not interfere directly with auxin action. This was confirmed *in vivo* by treatment of *p35S::DII-Venus* seedlings, when the exogenous application of 2,4-D in an equivalent amount to that produced from FluorA metabolism produced a similar response as FluorA treatment itself.

The presented fluorescent analogues FluorA I and FluorA II were mainly designed as tools for direct visualisation of auxin distribution *in planta*. Chemical biology and genetic approaches used to study the transport mechanisms of these compounds revealed that both of the FluorAs, to a greater extent compared with free 2,4-D, were able to bypass active auxin uptake into the cells due to the contribution of passive diffusion. It can be rationalised that attaching the linker-NBD hydrophobic moiety (Bertorelle *et al.*, 2002; Santa *et al.*, 2002) to the hydrophilic carboxyl group of 2,4-D significantly increased the hydrophobicity of the molecules and therefore improved their penetration across the lipid membranes. The different physico-chemical properties of FluorA compounds are likely to also explain the differences in the intensity of the fluorescence signal *in planta*. Indeed, fluorescently tagged compounds with different linker structures can significantly differ in their fluorescence intensity (Bielezová *et al.*, 2019). The further distribution of the compounds is proposed to be driven by mechanisms of active auxin transport. The increased fluorescence intensity of the FluorAs in both roots and hypocotyls after NPA treatment is consistent with findings that 2,4-D is a substrate for PIN and ABCB transporters (Petrášek *et al.*, 2006; Yang & Murphy, 2009; Hošek *et al.*, 2012). However, the accumulation of FluorAs in the root tip and hypocotyl after NPA treatment does not exactly resemble the effect of NPA on *pDR5::GUS* or *pDR5::GFP* seedlings, which alternatively results in accumulated DR5 response signal specifically around the QC in the distal root tip region (Sabatini *et al.*, 1999; Bailly *et al.*, 2008) and just below the cotyledons in the hypocotyl (Žádníková *et al.*, 2010). NPA is thought to enhance endogenous auxin accumulation at its sites of biosynthesis and/or localisation. However, FluorAs are likely to enter tissues over the entire seedling surface during the immersion treatment, which should lead to a different accumulation pattern following NPA treatment.

By contrast, POA-derived FluorA XI was not effectively taken up into the roots of Col-0. This corresponds with the fact that unsubstituted phenoxyacetic acid has a low lipid solubility, while addition of two chlorine atoms increases this solubility and therefore greatly supports the uptake of 2,4-D derivatives (Thimann, 1977). Furthermore, the PIP-NBD substructure lacking the 2,4-D part displayed no signal in the roots, confirming that the 2,4-D moiety was crucial for the uptake of the compounds into the plant.

In planta, the fluorescent 2,4-D conjugates mimicked the asymmetric distributions of auxin known to occur in Arabidopsis roots and shoots (Benková *et al.*, 2003; Friml, 2003; Žádníková *et al.*, 2010). The transport of auxin in lateral root primordia and young developing roots is an efflux-dependent process involving major roles of PIN1, ABCB1 and ABCB19 (Benková *et al.*,

2003; Zažímalová *et al.*, 2010), while the generation of auxin gradients in gravistimulated roots is driven mainly by PIN2 (Abas *et al.*, 2006; Rahman *et al.*, 2010) and PIN3 (Friml *et al.*, 2002) carriers. Taken together, the observed accumulations of FluorA I suggested that this compound is also actively transported by PIN or ABCB auxin carriers in the roots, lateral roots and gravistimulated primary roots of Arabidopsis.

The formation of the apical hook depends on asymmetric auxin distribution coordinated by the PIN1, 3, 4 and 7 auxin efflux carriers (Žádníková *et al.*, 2010). Light-stimulated redistribution (Liscum & Hangarter, 1993), as well as passive diffusion, of IAA away from the concave side of the hook (Vandenbussche *et al.*, 2010) then leads to apical hook opening. In this developmental process, FluorA II distribution was similar to the native auxin response (Žádníková *et al.*, 2010). Moreover, as it was shown that PIN3, 4 and 7 are expressed in the epidermis and cortex of the hypocotyl during the maintenance phase of hook development (Žádníková *et al.*, 2010), our observations of FluorA II accumulated in this region of the *pin3pin4pin7* transport mutant suggested that these PIN proteins are required for FluorA II to be asymmetrically distributed. In addition to the PIN transporters, the auxin influx carriers AUX1 and LAX3 also play an important role in apical hook development (Vandenbussche *et al.*, 2010). Although our results suggested that FluorA I and II were not primarily transported by the AUX and LAX influx carriers in roots, the opposite situation was observed in the apical hook. Based on the auxin distribution model in the apical hook, AUX1 is mainly localised in the epidermis of the hypocotyl, contributing to lateral and basipetal auxin redistribution (Žádníková *et al.*, 2010). The impaired uptake of FluorA II in the hypocotyl of *aux1-21lax3* resulted in the loss of FluorA II accumulation on the concave side of the apical hook, which suggested a role for active auxin influx carriers on FluorA II distribution in shoots. Moreover, the differences in uptake of FluorA II between Col-0 and *Ler* WTs is an interesting point to further investigate as different responses to auxin analogues between these two ecotypes have been observed previously (Vain *et al.*, 2019). Sánchez *et al.* (2018) showed that the development of primary roots varied considerably among Arabidopsis ecotypes at the cellular level, contributing to distinct root cellular dynamics. This might influence the import of chemicals to the cells. Hypothetically, as different ecotypes originate from different environmental conditions, Col-0 and *Ler* may have genetically encoded distinct properties and composition of the cuticle, cell wall or plasma membranes, resulting in different permeability and fluidity properties and consequently displaying differences in the uptake of the chemical substances.

We also observed that FluorA compounds localise in specific organelles, showing that both FluorA I and FluorA II are suitable for studies of auxin distribution at the subcellular level *in planta*. In agreement with the previous identification of ER-localised auxin transporters (Barbez *et al.*, 2012; Ding *et al.*, 2012; Simon *et al.*, 2016), both FluorAs displayed a strong co-localisation with an ER marker. We did not clearly detect FluorA compounds in the nucleus, however, which could be explained by a putative low auxin concentration within the nucleus, below the detection limit of the confocal imaging technique. Previously, the ER was shown

to play a dominant role in the regulation of nuclear auxin uptake (Middleton *et al.*, 2018). However, the regulatory mechanisms controlling free auxin levels in the nucleus are still unknown and multidisciplinary approaches combining tools such as auxin fluorescent probes and organelle sorting with sensitive MS-based methods could help to solve this matter. Interestingly, we also detected the presence of FluorAs in the endosomes of living plants. The localisation of auxin within the endomembrane system has been observed by invasive immunocytochemical staining in *Arabidopsis* and maize, in which IAA was detected in dictyosomes and cytoplasmic vesicles (Schlicht *et al.*, 2006; Metzbach *et al.*, 2017). Interestingly, PIN auxin transport carriers are localised both at the plasma membrane and in endosomes (Kleine-Vehn *et al.*, 2011). However, it remains unclear whether PIN carriers are only active at the plasma membrane or are also active at the endosome membranes, where they could facilitate the transport of auxin into these endosomes. Releasing the auxin content of endosome-derived vesicles upon fusion with the plasma membrane may contribute to the total flux of PAT (Baluška *et al.*, 2003) as indicated by Mancuso *et al.* (2007). Despite such vesicular secretion being theoretically refuted as a major mechanism of auxin transport *in planta* by mathematical modelling (Hille *et al.*, 2018), vesicle-based auxin exocytosis from single plant protoplasts has been detected and quantified by an amperometry method developed for real-time monitoring of vesicular IAA release (Liu *et al.*, 2014). Importantly, fluorescent auxin probes can help to reveal more about how the endomembrane system participates in intracellular and tissue-level auxin transport. Moreover, endosome isolation methods, such as organelle enrichment using endosome epitope-specific antibodies (Wilkop *et al.*, 2019) or fluorescent activated sorting of fluorescently labelled endosomes, coupled with MS detection, could provide precise quantification of auxin in pure endosomes and help to determine how the subcellular distribution contributes to the maintenance of cellular auxin homeostasis and plant development.

To conclude, although both FluorA I and II fluorescent conjugates of 2,4-D with NBD were shown to be inactive in auxin signalling, they mimicked the auxin distribution patterns known to occur *in planta* in distinct developmental processes. The structural modifications of the 2,4-D molecule altered the behaviour of the compounds compared with free 2,4-D. Therefore, despite being 2,4-D derivatives, FluorA compounds were able to bypass active auxin influx mechanisms by passive diffusion similarly to IAA. Moreover, they also appeared to be distributed efficiently via the auxin transport system with similar tissue-specific preferences as native auxin. FluorA I and II displayed potential as fluorescent auxin probes for visualisation of auxin distribution in the roots and apical hook, respectively. In the hook, a clear impact of active transport carriers on the distribution of FluorA II was demonstrated. Additionally, the light-stimulated redistribution of FluorA II from the zone of auxin maximum, mimicking auxin-like distribution, makes FluorA II a convenient tool to study PAT mechanisms during this developmental process. As low-molecular-mass compounds, FluorAs provide a subcellular resolution of visualisation, making them valuable tools for

following subcellular auxin gradients and studies of mechanisms for maintaining auxin intracellular homeostasis. In summary, the FluorA fluorescent 2,4-D compounds represent a convenient complementary research toolset to visualise and study the relationship between auxin action and localisation *in planta* at both tissue and subcellular levels.









Acknowledgements

We greatly thank Dolf Weijers and Che-Yang Liao for sharing the *pDR5v2::Venus* marker line seeds. We are thankful to Ota Blahoušek for technical assistance with editing of figures and Tomáš Pospíšil for providing stable isotope-labelled precursors for synthesis of internal FluorA standards. This work was supported by the Ministry of Education, Youth and Sports of the Czech Republic through the European Regional Development Fund-Project 'Plants as a tool for sustainable global development' (CZ.02.1.01/0.0/0.0/16_019/0000827), the Palacký University Olomouc Young Researcher grant no. JG_2020_002 (AŽ, BP), the Internal Grant Agency of Palacký University (IGA_PrF_2021_011), Vetenskapsrådet and VINNOVA (Verket för Innovationssystemet to TV, SRaggi, SMD, SRobert), Knut och Alice Wallenbergs Stiftelse via 'Shapesystem' grant no. 2012.0050 (SMD, SRobert), Kempestiftelserna (PG), the Carl Tryggers foundation (PG), the Swedish Research Council grant no. VR2016-00768 (PG), Olle Engkvist Byggnästars foundation grant 185 595 (SRaggi), the EU MSCA-IF project CrysPINs 792329 (MFKu) and the Endowment Fund of Palacký University in Olomouc (BP).

Author contributions

BP, AŽ, TV, PG, KD, SRobert and ON designed research; BP, AŽ, TV, PG, SRaggi, SRobert, MFKu and MKi performed research; BP, AŽ, TV, PG, SRaggi, MKu, M.Ki, MS, SK, RN, KD, SMD, SRobert and ON analysed data; BP, AŽ, SMD, SRobert and ON wrote the paper with contributions of all the authors; KD, SK, RN, MS, SRobert and ON supervised the research; BP, AŽ, TV and PG contributed equally to this work; all authors commented on the manuscript.

ORCID

Karel Doležal  <https://orcid.org/0000-0003-4938-0350>
 Siamsa M. Doyle  <https://orcid.org/0000-0003-4889-3496>
 Peter Grones  <https://orcid.org/0000-0003-4132-4151>
 Stefan Kepinski  <https://orcid.org/0000-0001-9819-5034>
 Martin Kieffer  <https://orcid.org/0000-0002-0987-2716>
 Martin F. Kuběš  <https://orcid.org/0000-0003-2182-4490>
 Richard Napier  <https://orcid.org/0000-0002-0605-518X>
 Ondřej Novák  <https://orcid.org/0000-0003-3452-0154>
 Barbora Pařízková  <https://orcid.org/0000-0002-8125-2271>
 Sara Raggi  <https://orcid.org/0000-0002-7925-5772>
 Stéphanie Robert  <https://orcid.org/0000-0002-0013-3239>
 Miroslav Strnad  <https://orcid.org/0000-0002-2806-794X>
 Thomas Vain  <https://orcid.org/0000-0002-8153-907X>
 Asta Žukauskaitė  <https://orcid.org/0000-0001-6759-8789>

Data availability

The data that support the findings of this study are available from the corresponding authors upon reasonable request.

References

- Abas L, Benjamins R, Malenica N, Paciorek T, Wiśniewska J, Moulinier-Anzola JC, Sieberer T, Friml J, Luschnig C. 2006. Intracellular trafficking and proteolysis of the Arabidopsis auxin-efflux facilitator PIN2 are involved in root gravitropism. *Nature Cell Biology* 8: 249–256.
- Abbas M, Alabadi D, Blázquez MA. 2013. Differential growth at the apical hook: all roads lead to auxin. *Frontiers in Plant Science* 4: 441.
- Adamowski M, Friml J. 2015. PIN-Dependent Auxin Transport: Action, Regulation, and Evolution. *Plant Cell* 27: 20–32.
- Atta S, Bera M, Chattopadhyay T, Paul A, Ikbāl M, Maiti MK, Pradeep Singh ND. 2015. Nano-pesticide formulation based on fluorescent organic photoresponsive nanoparticles: for controlled release of 2,4-D and real time monitoring of morphological changes induced by 2,4-D in plant systems. *RSC Advances* 5: 86990–86996.
- Atta S, Ikbāl M, Boda N, Gauri SS, Singh ND. 2013. Photoremovable protecting groups as controlled-release device for sex pheromone. *Photochemical and Photobiological Sciences* 12: 393–403.
- Atta S, Jana A, Ananthakrishnan R, Narayana Dhuleep PS. 2010. Fluorescent Caged Compounds of 2,4-Dichlorophenoxyacetic Acid (2,4-D): photorelease technology for controlled release of 2,4-D. *Journal of Agricultural and Food Chemistry* 58: 11844–11851.
- Bailly A, Sovero V, Vincenzetti V, Santelia D, Bartnik D, Koenig BW, Mancuso S, Martinoia E, Geisler M. 2008. Modulation of P-glycoproteins by auxin transport inhibitors is mediated by interaction with immunophilins. *Journal of Biological Chemistry* 283: 21817–21826.
- Baluška F, Šamaj J, Menzel D. 2003. Polar transport of auxin: carrier-mediated flux across the plasma membrane or neurotransmitter-like secretion? *Trends in Cell Biology* 13: 282–285.
- Barbez E, Kubeš M, Rolčík J, Béziat C, Pěncík A, Wang B, Rosquete MR, Zhu J, Dobrev PI, Lee Y *et al.* 2012. A novel putative auxin carrier family regulates intracellular auxin homeostasis in plants. *Nature* 485: 119–122.
- Benková E, Michniewicz M, Sauer M, Teichmann T, Seifertová D, Jürgens G, Friml J. 2003. Local, efflux-dependent auxin gradients as a common module for plant organ formation. *Cell* 115: 591–602.
- Bennett MJ, Marchant A, Green HG, May ST, Ward SP, Millner PA, Walker AR, Schulz B, Feldmann KA. 1996. *Arabidopsis* AUX1 gene: a permease-like regulator of root gravitropism. *Science* 273: 948–950.
- Bertorelle F, Dondon R, Fery-Forgues S. 2002. Compared behavior of hydrophobic fluorescent NBD probes in micelles and in cyclodextrins. *Journal of Fluorescence* 12: 205–207.
- Bielešová K, Pařízková B, Kubeš M, Husíková A, Kubala M, Ma Q, Sedlářová M, Robert S, Doležal K, Strnad M *et al.* 2019. New fluorescently labeled auxins exhibit promising anti-auxin activity. *New Biotechnology* 48: 44–52.
- Brunoud G, Wells DM, Oliva M, Larrieu A, Mirabet V, Burrow AH, Beekman T, Kepinski S, Traas J, Bennett MJ *et al.* 2012. A novel sensor to map auxin response and distribution at high spatio-temporal resolution. *Nature* 482: 103–106.
- Cho M, Lee SH, Cho HT. 2007. P-glycoprotein4 displays auxin efflux transporter-like action in *Arabidopsis* root hair cells and tobacco cells. *Plant Cell* 19: 3930–3943.
- Delbarre A, Muller P, Imhoff V, Guern J. 1996. Comparison of mechanisms controlling uptake and accumulation of 2,4-dichlorophenoxy acetic acid, naphthalene-1-acetic acid, and indole-3-acetic acid in suspension-cultured tobacco cells. *Planta* 198: 532–541.
- Ding X, Wang B, Moreno I, Dupláková N, Simon S, Carraro N, Reemmer J, Pěncík A, Chen X, Tejos R *et al.* 2012. ER-localized auxin transporter PIN8 regulates auxin homeostasis and male gametophyte development in *Arabidopsis*. *Nature Communications* 3: 941.
- Enders TA, Strader LC. 2016. Auxin activity: past, present, and future. *American Journal of Botany* 102: 180–196.
- Eyer L, Vain T, Pařízková B, Oklestkova J, Barbez E, Kozubíková H, Pospíšil T, Wierzbicka R, Kleine-Vehn J, Fránek M *et al.* 2016. 2,4-D and IAA amino acid conjugates show distinct metabolism in *Arabidopsis*. *PLoS ONE* 11: e0159269.
- Friml J. 2003. Auxin transport—shaping the plant. *Current Opinion in Plant Biology* 6: 7–12.
- Friml J, Wiśniewska J, Benková E, Mendgen K, Palme K. 2002. Lateral relocation of auxin efflux regulator PIN3 mediates tropism in *Arabidopsis*. *Nature* 415: 806–809.
- Geisler M, Murphy AS. 2006. The ABC of auxin transport: The role of p-glycoproteins in plant development. *FEBS Letters* 580: 1094–1102.
- Grones P, Friml J. 2015. Auxin transporters and binding proteins at a glance. *Journal of Cell Science* 128: 1–7.
- Grossmann K. 2009. Auxin herbicides: current status of mechanism and mode of action. *Pest Management Science* 66: 113–120.
- Hayashi K, Nakamura S, Fukunaga S, Nishimura T, Jenness MK, Murphy AS, Motose H, Nozaki H, Furutani M, Aoyama T. 2014. Auxin transport sites are visualized in planta using fluorescent auxin analogs. *Proceedings of the National Academy of Sciences, USA* 111: 11557–11562.
- Hille S, Akhmanova M, Glanc M, Johnson A, Friml J. 2018. Relative contribution of PIN-containing secretory vesicles and plasma membrane PINs to the directed auxin transport: theoretical estimation. *International Journal of Molecular Sciences* 19: 3566.
- Hošek P, Kubeš M, Lanková M, Dobrev PI, Klíma P, Kohoutová M, Petrášek J, Hoyerová K, Jirina M, Zažimalová E. 2012. Auxin transport at cellular level: new insights supported by mathematical modelling. *Journal of Experimental Botany* 63: 3815–3827.
- Hoyerová K, Hošek P, Quareshy M, Li J, Klíma P, Kubeš M, Yemm AA, Neve P, Tripathi A, Bennett MJ *et al.* 2018. Auxin molecular field maps define AUX1 selectivity: many auxin herbicides are not substrates. *New Phytologist* 217: 1625–1639.
- Kamimoto Y, Terasaka K, Hamamoto M, Takanashi K, Fukuda S, Shitan N, Sugiyama A, Suzuki H, Shibata D, Wang B *et al.* 2012. *Arabidopsis* ABCB21 is a facultative auxin importer/exporter regulated by cytoplasmic auxin concentration. *Plant and Cell Physiology* 53: 2090–2100.
- Kleine-Vehn J, Wabnik K, Martinière A, Langowski Ł, Willig K, Naramoto S, Leitner J, Tanaka H, Jakobs S, Robert S *et al.* 2011. Recycling, clustering, and endocytosis jointly maintain PIN auxin carrier polarity at the plasma membrane. *Molecular Systems Biology* 7: 540.
- Kubeš M, Yang H, Richter GL, Cheng Y, Młodzińska E, Wang X, Blakeslee JJ, Carraro N, Petrášek J, Zažimalová E *et al.* 2012. The *Arabidopsis* concentration-dependent influx/efflux transporter ABCB4 regulates cellular auxin levels in the root epidermis. *The Plant Journal* 69: 640–654.
- Lace B, Prandi C. 2016. Shaping small bioactive molecules to untangle their biological function: a focus on fluorescent plant hormones. *Molecular Plant* 9: 1099–1118.
- Lavy M, Estelle M. 2016. Mechanisms of auxin signaling. *Development* 143: 3226–3229.
- Lee S, Sundaram S, Armitage L, Evans JP, Hawkes T, Kepinski S, Ferro N, Napier RM. 2014. Defining binding efficiency and specificity of auxins for SCF(TIR1/AFB)-Aux/IAA co-receptor complex formation. *ACS Chemical Biology* 9: 673–682.
- Lehman A, Black R, Ecker JR. 1996. HOOKLESS1, an ethylene response gene, is required for differential cell elongation in the *Arabidopsis* hypocotyl. *Cell* 85: 183–194.
- Lewis DR, Muday GK. 2009. Measurement of auxin transport in *Arabidopsis thaliana*. *Nature Protocols* 4: 437–451.
- Liscum E, Hangarter RP. 1993. Light-stimulated apical hook opening in wild-type *Arabidopsis thaliana* seedlings. *Plant Physiology* 101: 567–572.
- Liu JT, Hu LS, Liu YL, Chen RS, Cheng Z, Chen SJ, Amatore C, Huang WH, Huo KF. 2014. Real-time monitoring of auxin vesicular exocytotic efflux from single plant protoplasts by amperometry at microelectrodes decorated with nanowires. *Angewandte Chemie International Edition* 53: 2643–2647.
- Ljung K. 2013. Auxin metabolism and homeostasis during plant development. *Development* 140: 943–950.
- Lomax TL, Muday GK, Rubery PH. 1995. Auxin transport. In: Davies PJ, ed. *Plant hormones*. Dordrecht, Netherlands: Springer, 509–530.

- Ludwig-Müller J. 2011. Auxin conjugates: their role for plant development and in the evolution of land plants. *Journal of Experimental Botany* 62: 1757–1773.
- Ma Q, Robert S. 2014. Auxin biology revealed by small molecules. *Physiologia Plantarum* 151: 25–42.
- Mancuso S, Marras AM, Mugnai S, Schlicht M, Žárský V, Li G, Song L, Xue HW, Baluška F. 2007. Phospholipase D ζ 2 drives vesicular secretion of auxin for its polar cell-cell transport in the transition zone of the root apex. *Plant Signaling & Behavior* 2: 240–244.
- Mao H, Nakamura M, Viotti C, Grebe M. 2016. A framework for lateral membrane trafficking and polar tethering of the PEN3 ATP-binding cassette transporter. *Plant Physiology* 172: 2245–2260.
- Marin E, Jouannet V, Herz A, Lokerse AS, Weijers D, Vaucheret H, Nussbaum L, Crespi MD, Maizel A. 2010. miR390, Arabidopsis TAS3 tasiRNAs, and their AUXIN RESPONSE FACTOR targets define an autoregulatory network quantitatively regulating lateral root growth. *Plant Cell* 22: 1104–1117.
- Metzbach U, Strnad M, Mancuso S, Baluška F. 2017. Immunogold-EM analysis reveal brefeldin a-sensitive clusters of auxin in *Arabidopsis* root apex cells. *Communicative & Integrative Biology* 10: e1327105.
- Middleton AM, Dal Bosco C, Chlap P, Bensch R, Harz H, Ren F, Bergmann S, Wend S, Weber W, Hayashi KI *et al.* 2018. Data-driven modeling of intracellular auxin fluxes indicates a dominant role of the ER in controlling nuclear auxin uptake. *Cell Reports* 22: 3044–3057.
- Mitchison G. 2015. The Shape of an Auxin Pulse, and What It Tells Us about the Transport Mechanism. *PLoS Computational Biology* 11: e1004487.
- Montesinos JC, Sturm S, Langhans M, Hillmer S, Marcote MJ, Robinson DG, Aniento F. 2012. Coupled transport of Arabidopsis p24 proteins at the ER-Golgi interface. *Journal of Experimental Botany* 63: 4243–4261.
- Muscolo A, Sidari M, Francioso O, Tugnoli V, Nardi S. 2007. The auxin-like activity of humic substances is related to membrane interactions in carrot cell cultures. *Journal of Chemical Ecology* 33: 115–129.
- Pařízková B, Pernisová M, Novák O. 2017. What has been seen cannot be unseen – detecting auxin *in vivo*. *International Journal of Molecular Sciences* 18: 2736.
- Péret B, Swarup K, Ferguson A, Seth M, Yang Y, Dhondt S, James N, Casimiro I, Perry P, Syed A, *et al.* 2012. AUX/LAX genes encode a family of auxin influx transporters that perform distinct functions during *Arabidopsis* development. *Plant Cell* 24: 2874–2885.
- Petráček J, Friml J. 2009. Auxin transport routes in plant development. *Development* 136: 2675–2688.
- Petráček J, Mravec J, Bouchard R, Blakeslee JJ, Abas M, Seifertová D, Wisniewska J, Tadele Z, Kubeš M, Covanová M *et al.* 2006. PIN proteins perform a rate-limiting function in cellular auxin efflux. *Science* 312: 914–918.
- Rahman A, Takahashi M, Shibasaki K, Wu S, Inaba T, Tsurumi S, Baskin TI. 2010. Gravitropism of *Arabidopsis thaliana* roots requires the polarization of PIN2 toward the root tip in meristematic cortical cells. *Plant Cell* 22: 1762–1776.
- Ranocha P, Dima O, Nagy R, Felten J, Corratgé-Faillie C, Novák O, Morreel K, Lacombe B, Martinez Y, Pfrunder S *et al.* 2013. *Arabidopsis* WAT1 is a vacuolar auxin transport facilitator required for auxin homeostasis. *Nature Communications* 4: 2625.
- Robert S, Chary SN, Drakakaki G, Li S, Yang Z, Raikhel NV, Hicks GR. 2008. Endosidin1 defines a compartment involved in endocytosis of the brassinosteroid receptor BRI1 and the auxin transporters PIN2 and AUX1. *Proceedings of the National Academy of Sciences, USA* 105: 8464–8469.
- Sabatini S, Beis D, Wolkenfeld H, Murfett J, Guilfoyle T, Malamy J, Benfey P, Leyser O, Bechtold N, Weisbeek P *et al.* 1999. An auxin-dependent distal organizer of pattern and polarity in the *Arabidopsis* root. *Cell* 99: 463–472.
- Sánchez WC, García-Ponce B, de la Paz SM, Álvarez-Buylla ER. 2018. Identifying the transition to the maturation zone in three ecotypes of *Arabidopsis thaliana* roots. *Communicative & Integrative Biology* 11: e1395993.
- Santa T, Matsumura D, Huang CZ, Kitada C, Imai K. 2002. Design and synthesis of a hydrophilic fluorescent derivatization reagent for carboxylic acids, 4-N-(4-N-aminoethyl)piperazino-7-nitro-2,1,3-benzoxadiazole (NBD-PZ-NH₂), and its application to capillary electrophoresis with laser-induced fluorescence detection. *Biomedical Chromatography* 16: 523–528.
- Sauer M, Robert S, Kleine-Vehn J. 2013. Auxin: simply complicated. *Journal of Experimental Botany* 64: 2565–2577.
- Schindelin J, Rueden CT, Hiner MC, Eliceiri KW. 2015. The ImageJ ecosystem: An open platform for biomedical image analysis. *Molecular Reproduction and Development* 82: 518–529.
- Schlicht M, Strnad M, Scanlon MJ, Mancuso S, Hochholdinger F, Palme K, Volkmann D, Menzel D, Baluška F. 2006. Auxin immunolocalization implicates vesicular neurotransmitter-like mode of polar auxin transport in root apices. *Plant Signaling & Behavior* 1: 122–133.
- Schwark A, Schierle J. 1992. Interaction of ethylene and auxin in the regulation of hook growth I: the role of auxin in different growing regions of the hypocotyl hook of *Phaseolus vulgaris*. *Journal of Plant Physiology* 140: 562–570.
- Seifertová D, Skůpa P, Rychtář J, Laňková M, Pařezová M, Dobrev PI, Hoyerová K, Petráček J, Zažímalová E. 2014. Characterization of transmembrane auxin transport in *Arabidopsis* suspension-cultured cells. *Journal of Plant Physiology* 171: 429–437.
- Simon S, Petráček J. 2010. Why plants need more than one type of auxin. *Plant Science* 180: 454–460.
- Simon S, Skůpa P, Viae T, Zwiewka M, Tejos R, Klíma P, Černá M, Rolčík J, De Rycke R, Moreno I *et al.* 2016. PIN6 auxin transporter at endoplasmic reticulum and plasma membrane mediates auxin homeostasis and organogenesis in *Arabidopsis*. *New Phytologist* 211: 65–74.
- Skalický V, Kubeš M, Napier R, Novák O. 2018. Auxins and cytokinins—the role of subcellular organization on homeostasis. *International Journal of Molecular Sciences* 19: 3115.
- Sokolowska K, Kizińska J, Szewczuk Z, Banasiak A. 2014. Auxin conjugated to fluorescent dyes—a tool for the analysis of auxin transport pathways. *Plant Biology* 16: 866–877.
- Steinmann T, Geldner N, Grebe M, Mangold S, Jackson CL, Paris S, Gälweiler L, Palme K, Jürgens G. 1999. Coordinated polar localization of auxin efflux carrier PIN1 by GNOM ARF GEF. *Science* 286: 316–318.
- Swarup K, Benková E, Swarup R, Casimiro I, Péret B, Yang Y, Parry G, Nielsen E, De Smet I, Vanneste S *et al.* 2008. The auxin influx carrier LAX3 promotes lateral root emergence. *Nature Cell Biology* 10: 946–954.
- Tan X, Calderon-Villalobos LI, Sharon M, Zheng C, Robinson CV, Estelle M, Zheng N. 2007. Mechanism of auxin perception by the TIR1 ubiquitin ligase. *Nature* 446: 640–645.
- Thimann KV. 1977. *Hormone action in the whole life of plants*. Amherst, MA, USA: University of Massachusetts Press.
- Tsuda E, Yang H, Nishimura T, Uehara Y, Sakai T, Furutani M, Koshiba T, Hirose M, Nozaki H, Murphy AS *et al.* 2011. Alkoxy-auxins are selective inhibitors of auxin transport mediated by PIN, ABCB, and AUX1 transporters. *Journal of Biological Chemistry* 286: 2354–2364.
- Ulmasov T, Hagen G, Guilfoyle TJ. 1997. ARF1, a transcription factor that binds to auxin response elements. *Science* 276: 1865–1868.
- Vain T, Raggi S, Ferro N, Barange DK, Kieffer M, Ma Q, Doyle SM, Thelander M, Pařízková B, Novák O *et al.* 2019. Selective auxin agonists induce specific AUX/IAA protein degradation to modulate plant development. *Proceedings of the National Academy of Sciences, USA* 116: 6463–6472.
- Vandenbussche F, Petráček J, Žádníková P, Hoyerová K, Pešek B, Raz V, Swarup R, Bennett M, Zažímalová E, Benková E *et al.* 2010. The auxin influx carriers AUX1 and LAX3 are involved in auxin-ethylene interactions during apical hook development in *Arabidopsis thaliana* seedlings. *Development* 137: 597–606.
- Vanneste S, Friml J. 2009. Auxin: a trigger for change in plant development. *Cell* 136: 1005–1016.
- Vieten A, Sauer M, Brewer PB, Friml J. 2007. Molecular and cellular aspects of auxin-transport-mediated development. *Trends in Plant Science* 12: 160–168.
- Wilkop T, Pattathil S, Ren G, Davis DJ, Bao W, Duan D, Peralta AG, Domozych DS, Hahn MG, Drakakaki G. 2019. A hybrid approach enabling large-scale glycomic analysis of post-golgi vesicles reveals a transport route for polysaccharides. *Plant Cell* 31: 627–644.
- Woodward AW, Bartel B. 2005. Auxin: regulation, action, and interaction. *Annals of Botany* 95: 707–735.
- Yang H, Murphy AS. 2009. Functional expression and characterization of *Arabidopsis* ABCB, AUX1 and PIN auxin transporters in *Schizosaccharomyces pombe*. *The Plant Journal* 59: 179–191.

Yang Y, Hammes UZ, Taylor CG, Schachtman DP, Nielsen E. 2006. High-affinity auxin transport by the AUX1 influx carrier protein. *Current Biology* 16: 1123–1127.

Žádníková P, Petrášek J, Marhavý P, Raz V, Vandenbussche F, Ding Z, Schwarzerová K, Morita MT, Tasaka M, Hejácíko J. 2010. Role of PIN-mediated auxin efflux in apical hook development of *Arabidopsis thaliana*. *Development* 137: 607–617.

Zážímalová E, Murphy AS, Yang H, Hoyerová K, Hošek P. 2010. Auxin transporters—why so many? *Cold Spring Harbor Perspectives in Biology* 2: a001552.

Supporting Information

Additional Supporting Information may be found online in the Supporting Information section at the end of the article.

Dataset S1 Raw data obtained from surface plasmon resonance (SPR) binding analysis of FluorA compounds to auxin receptor.

Fig. S1 Library of fluorescent auxin analogues and scheme of screening strategy that was used for selecting the best candidates.

Fig. S2 Testing of the biological activity of the FluorA compounds in auxin-related bioassays.

Fig. S3 Concentration and time-dependent accumulation of selected FluorA compounds.

Fig. S4 Distribution of FluorA compounds *in planta*.

Fig. S5 Tissue-specific distribution response of FluorA II to light in apical hook.

Fig. S6 Subcellular localisation of FluorA XI.

Methods S1 Synthesis of FluorA compounds.

Methods S2 LC-MS/MS determination of metabolisation dynamics.

Methods S3 GUS assay.

Methods S4 Surface plasmon resonance (SPR).

Methods S5 FluorA transport assay and subcellular localisation imaging.

Notes S1 Storage and usage of the compounds.

Table S1 Quantification of *Arabidopsis* primary root length after 5 d of treatment with FluorA compounds.

Table S2 Uptake and metabolisation of FluorA compounds *in planta* determined by sensitive liquid chromatography–mass spectrometry (LC-MS) detection.

Table S3 LC-MS determination of 2,4-D uptake to *Arabidopsis* roots after treatment of *Arabidopsis* seedlings with increasing 2,4-D concentrations.

Table S4 Biological activity of FluorA compounds estimated by the quantification of Venus fluorescence signal in *p35S::DII-Venus* *Arabidopsis* seedlings in response to FluorA treatment.

Table S5 Effect of active auxin efflux on FluorA distribution in primary root of *Arabidopsis thaliana*.

Table S6 Effect of active auxin influx on FluorA uptake in primary root of *Arabidopsis thaliana*.

Please note: Wiley Blackwell are not responsible for the content or functionality of any Supporting Information supplied by the authors. Any queries (other than missing material) should be directed to the *New Phytologist* Central Office.